Short Article

Cell Stem Cell

Tissue-Engineered Vascular Grafts with Advanced Mechanical Strength from Human iPSCs

Graphical Abstract

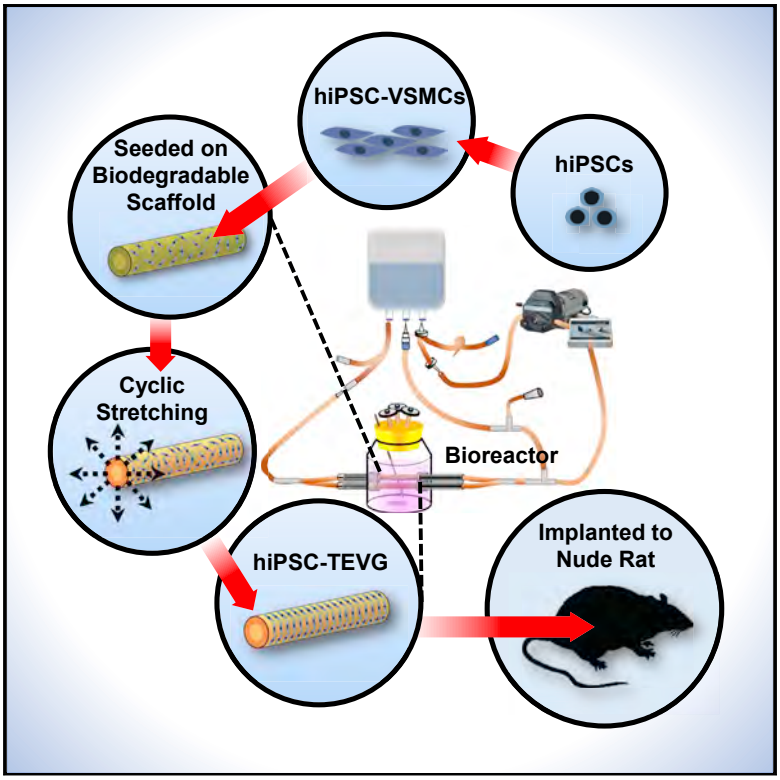

Authors

Jiesi Luo, Lingfeng Qin, Liping Zhao, ..., Alan Dardik, Laura E. Niklason, Yibing Qyang

Correspondence

yibing.qyang@yale.edu

In Brief

Luo et al. generated tissue-engineered vascular grafts (TEVGs) using human induced pluripotent stem cell (hiPSC)-derived vascular smooth muscle cells. These hiPSC-derived TEVGs displayed mechanical strength comparable to that of native vessels used clinically as vascular grafts and maintained excellent patency and mechanical function following implantation into a rat model.

Highlights

- Functional VSMCs could be efficiently generated on a large scale from hiPSCs
- Optimized biochemical and biophysical conditions were used to generate hiPSC-TEVGs
- hiPSC-TEVGs presented mechanical strength comparable to that of saphenous veins
- hiPSC-TEVGs maintained patency and mechanical function following rat implantation

Luo et al., 2020, Cell Stem Cell *26*, 1–11
February 6, 2020
https://doi.org/10.1016/j.stem.2019.12.012

CellPress

Please cite this article in press as: Luo et al., Tissue-Engineered Vascular Grafts with Advanced Mechanical Strength from Human iPSCs, Cell Stem Cell (2020), https://doi.org/10.1016/j.stem.2019.12.012

Cell Stem Cell
Short Article

Tissue-Engineered Vascular Grafts with Advanced Mechanical Strength from Human iPSCs

Jiesi Luo,[1,2] Lingfeng Qin,[3] Liping Zhao,[4,5] Liqiong Gui,[4,5] Matthew W. Ellis,[1,2,6] Yan Huang,[1,2] Mehmet H. Kural,[4,5] J. Alexander Clark,[7] Shun Ono,[3,4] Juan Wang,[4,5] Yifan Yuan,[4,5] Shang-Min Zhang,[8] Xiaoqiang Cong,[1,2,9] Guangxin Li,[3,10] Muhammad Riaz,[1,2] Colleen Lopez,[1,2] Akitsu Hotta,[11] Stuart Campbell,[7] George Tellides,[3,4] Alan Dardik,[3,4] Laura E. Niklason,[2,4,5,7] and Yibing Qyang[1,2,4,8,12,*]

[1]Yale Cardiovascular Research Center, Section of Cardiovascular Medicine, Department of Internal Medicine, Yale School of Medicine, New Haven, CT 06511, USA
[2]Yale Stem Cell Center, New Haven, CT 06520, USA
[3]Department of Surgery, Yale University, New Haven, CT 06520, USA
[4]Vascular Biology and Therapeutics Program, Yale University School of Medicine, New Haven, CT 06520, USA
[5]Department of Anesthesiology, Yale University, New Haven, CT 06519, USA
[6]Department of Cellular and Molecular Physiology, Yale University, New Haven, CT 06519, USA
[7]Department of Biomedical Engineering, Yale University, New Haven, CT 06519, USA
[8]Department of Pathology, Yale School of Medicine, New Haven, CT 06520, USA
[9]Department of Cardiology, Bethune First Hospital of Jilin University, ChangChun 130021, China
[10]Department of Vascular Surgery, The First Hospital of China Medical University, Shenyang 110122, China
[11]Center for iPS Cell Research and Application (CiRA), Kyoto University, Kyoto 606-8501, Japan
[12]Lead Contact
*Correspondence: yibing.qyang@yale.edu
https://doi.org/10.1016/j.stem.2019.12.012

SUMMARY

Vascular smooth muscle cells (VSMCs) can be derived in large numbers from human induced pluripotent stem cells (hiPSCs) for producing tissue-engineered vascular grafts (TEVGs). However, hiPSC-derived TEVGs are hampered by low mechanical strength and significant radial dilation after implantation. Here, we report generation of hiPSC-derived TEVGs with mechanical strength comparable to native vessels used in arterial bypass grafts by utilizing biodegradable scaffolds, incremental pulsatile stretching, and optimal culture conditions. Following implantation into a rat aortic model, hiPSC-derived TEVGs show excellent patency without luminal dilation and effectively maintain mechanical and contractile function. This study provides a foundation for future production of non-immunogenic, cellularized hiPSC-derived TEVGs composed of allogenic vascular cells, potentially serving needs to a considerable number of patients whose dysfunctional vascular cells preclude TEVG generation via other methods.

INTRODUCTION

Mechanically robust vascular grafts are in urgent clinical demand for treating cardiovascular diseases or providing hemodialysis access. While autologous or synthetic vascular grafts are clinically employed, the lack of suitable native vessels from patients or the potential risk of thrombosis and infection from synthetic materials hampers their application and efficacy (Akoh and Patel, 2010; Conte, 2013). The application of human allograft vessels from cadavers (Madden et al., 2005) has also been reported. However, potential aneurysm, calcification, and thrombosis hinder their widespread clinical utilization. Tissue-engineered vascular grafts (TEVGs) provide an alternative source of vascular grafts, and TEVGs with remarkable mechanical strength have been generated from human primary vascular smooth muscle cells (VSMCs) or fibroblasts (Dahl et al., 2011; McAllister et al., 2009; Syedain et al., 2017). To date, TEVGs from primary VSMCs coupled with decellularization have achieved promising results for hemodialysis access in clinical trials (Lawson et al., 2016). Acellular TEVGs, therefore, offer a readily available option for emergent vascular intervention (Elliott et al., 2019; Lawson et al., 2016; Wu et al., 2012) but should also allow for effective ingrowth and vascular remodeling for long-term engraftment and ultimate replacement of the implanted graft by host vascular tissue. However, vascular cells from a substantial number of patients who may need TEVGs could have defective proliferation or vascular remodeling due to advanced age or diseases such as diabetes (Poh et al., 2005; Spinetti et al., 2008) and as a result may not benefit from acellular TEVGs. As such, current acellular TEVGs may not work efficaciously for a considerable patient population in need.

Alternatively, human induced pluripotent stem cells (hiPSCs) may fundamentally address the above challenges (Song et al., 2018). hiPSCs, derived from reprogramming somatic cells by ectopic expression of stem cell factors (Takahashi et al., 2007), are self-renewable and capable of differentiating into virtually any cell type in the body, including VSMCs. VSMCs have previously been generated from hiPSCs (hiPSC-VSMCs) and used for tissue fabrication and disease modeling (Atchison et al., 2017; Bajpai et al., 2012; Cheung et al., 2012; Dash et al., 2016; Eoh et al., 2017; Patsch et al., 2015; Wang et al., 2014). Moreover,

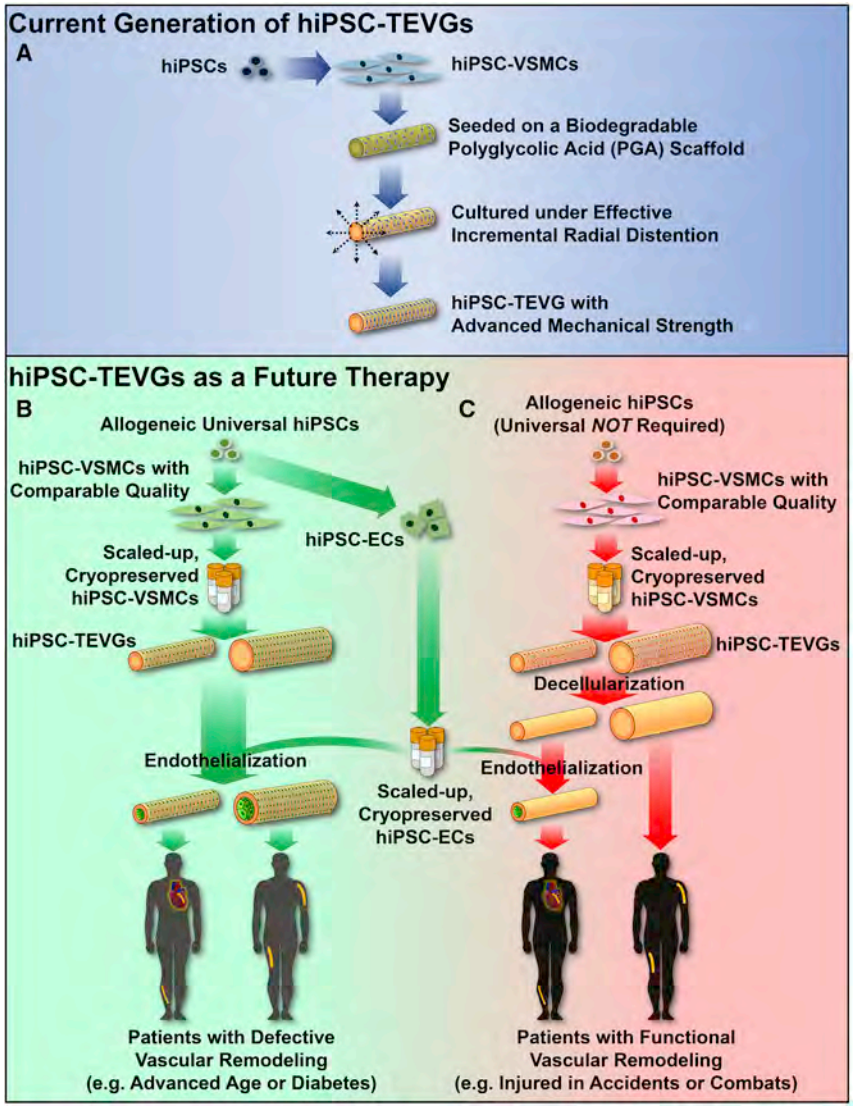

Figure 1. Strategies for Generating hiPSC-Based TEVGs

Current generation of hiPSC-TEVGs (A) and strategies for hiPSC-TEVGs as a future therapy (B and C). For small-diameter (2–4 mm) bypass applications (e.g., coronary artery or below the knee), allogeneic, universal hiPSC-ECs would be used to coat the grafts to prevent coagulation and luminal stenosis before implantation. Large-diameter (≥6 mm) TEVGs could be immediately available for vascular intervention without the need for endothelialization (e.g., above the knee or hemodialysis). Note that short-term storage and multi-site coordination for graft production and usage based on estimated clinical need are feasible and necessary for cells containing TEVG applications in (B) and (C).

recent studies reported that "universal" or immunocompatible pluripotent stem cells can be produced by modulating the expression of human leukocyte antigens (HLAs) (Deuse et al., 2019; Gornalusse et al., 2017; Xu et al., 2019). This theoretically makes it possible to establish minimal or non-immunogenic hiPSC lines, with the ultimate goal of allowing allogeneic transplantation of hiPSC-derived tissue immunocompatible to any patient recipient. Thus, with the support of short-term storage for live tissue and multi-site manufacturing coordination, TEVGs generated on a large scale from universal hiPSC-VSMCs could provide promptly available, functional cell-based vascular grafts for patients with defective vascular remodeling in the future. To date, hiPSC-derived TEVGs (hiPSC-TEVGs) have been reported, but their continued development encountered a major obstacle in low mechanical strength and causative radial dilation in a rat aortic transplantation model (Gui et al., 2016) and would therefore not qualify for clinical transplantation. Thus, augmentation of mechanical strength is a priority before the future clinical application of hiPSC-TEVGs.

Herein, we cultured hiPSC-VSMCs onto biodegradable polyglycolic acid (PGA) scaffolds and developed hiPSC-TEVGs with remarkable mechanical strength approaching that of native vessels applied as typical arterial bypass grafts. The mechanical properties of TEVGs can be heightened by mechanical stretching to enhance collagen synthesis and proliferation of VSMCs (Kim et al., 1999; Niklason et al., 1999). We found that the incremental addition of pulsatile radial stress at 110–120 beats per minute (bpm) significantly heightened the mechanical properties of hiPSC-TEVGs (Figure 1A). Moreover, after a 4-week implantation as an interpositional aortic graft in a nude rat model, our hiPSC-TEVGs remained patent, without radial dilation, longitudinal elongation, or teratoma formation. Our current, mechanically robust hiPSC-TEVGs provide a critical foundation for addressing patients with defective vascular remodeling and pave the way for the production of universal hiPSC-TEVGs in the future as promptly available therapies (Figure 1B). Additionally, for patients with functional vascular remodeling, functionally comparable hiPSC-VSMCs could be produced and stocked on a large scale, eliminating the donor-donor functional variability of primary cells, which could allow for more efficient production of decellularized hiPSC-TEVGs as an off-the-shelf therapy (Figure 1C).

RESULTS

Robust, Large-Scale Generation of Functional hiPSC-VSMCs

Generation of hiPSC-TEVGs requires the large-scale production of hiPSC-VSMCs (Figure 1). We first optimized a method of deriving hiPSC-VSMCs (Figure S1A). In comparison with previous dispase-assisted embryoid body (EB) formation, more uniform EBs with healthier morphology were derived by EDTA-mediated hiPSC dissociation coupled with an extended medium

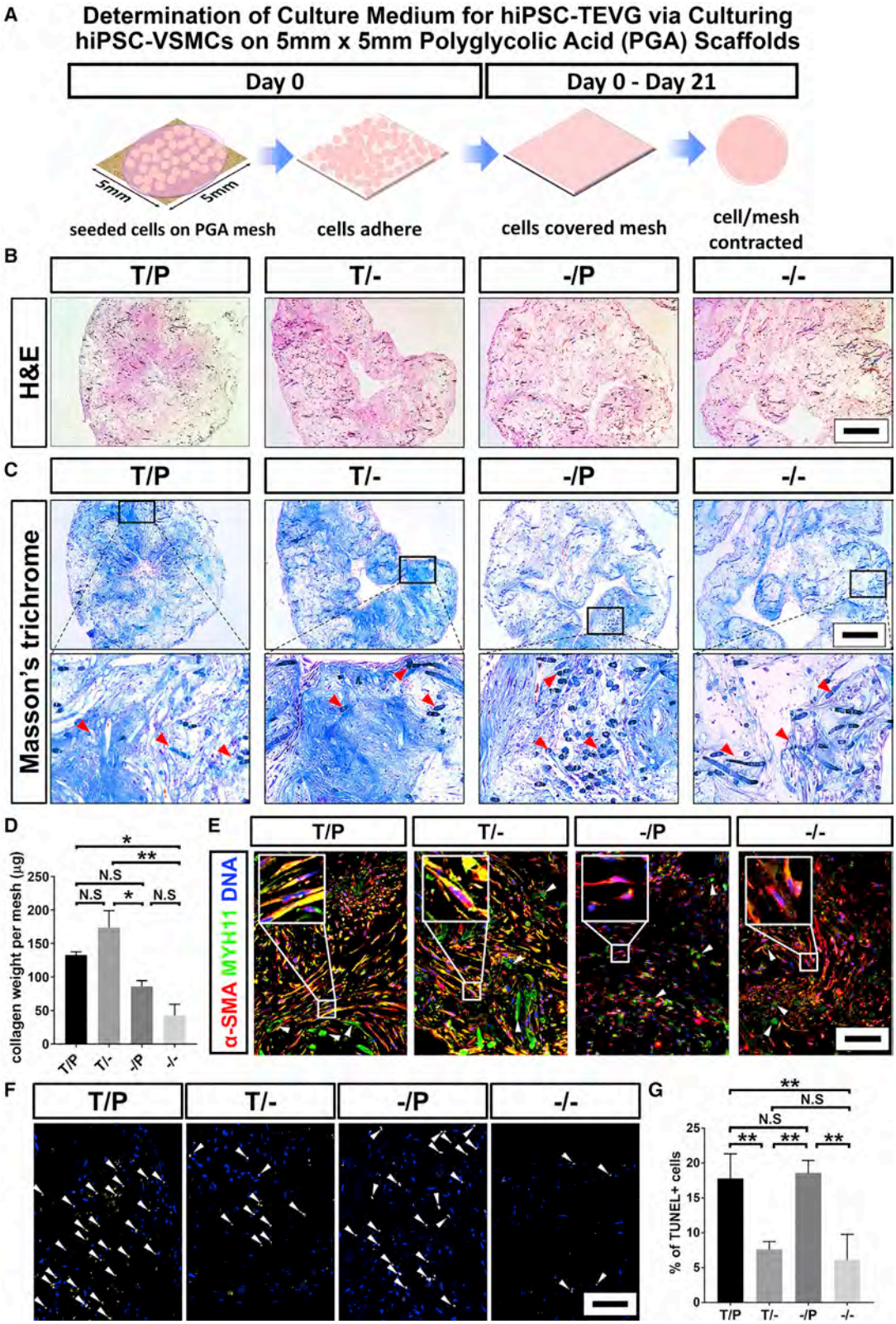

(legend on next page)

transition from mTeSR1 (hiPSC self-renewal medium) to EB differentiation medium (Figure S1B; details see STAR Methods). After 7–10 days of culture in SmGM-2 (VSMC growth medium), hiPSC-VSMCs in a proliferative state were derived (hiPSC-VSMCs-P). To validate VSMC properties, hiPSC-VSMCs-P were induced into a mature phenotype (hiPSC-VSMCs-M) by a maturation medium. Similar to human primary VSMCs, hiPSC-VSMCs-M exhibited higher expression levels of VSMC markers, including α-smooth muscle actin (α-SMA), calponin (CNN1), and smooth muscle myosin heavy chain (MYH11), as well as extracellular matrix (ECM) markers such as collagen type I (COL1) and elastin (ELN), compared with hiPSC-VSMCs-P (Figures S1C–S1E). hiPSC-VSMCs did not express OCT4, while hiPSCs were OCT4 positive but VSMC marker negative (Figures S1C–S1E). In addition, hiPSC-VSMCs following maturation significantly reduced cell surface area in response to vasoconstrictor (carbachol), indicating their functional contractility (Figures S1F and S1G). As expected, hiPSC-VSMCs-M showed increased contractility compared with hiPSC-VSMCs-P.

As growth factors like fibroblast growth factor 2 (FGF2) and epidermal growth factor (EGF) in SmGM-2 medium may reduce VSMC contractile function and collagen production (Chen et al., 2016; Schlumberger et al., 1991), both of which are essential for vascular graft engineering, we "primed" hiPSC-VSMCs-P in DMEM containing 10% fetal bovine serum (FBS) without exogenous FGF2 or EGF and named them generation 2 (Gen 2) hiPSC-VSMCs-10% FBS (Figure S1H). Gen 2 hiPSC-VSMCs-10% FBS showed an enhanced expression of VSMC and ECM markers but a similar growth rate compared with hiPSC-VSMCs-P (Figures S1H–S1J). In addition, compared with the Gen 1 hiPSC-VSMCs obtained via our previous approach (Gui et al., 2016), Gen 2 hiPSC-VSMCs-10% FBS exhibited a higher proliferative rate and an enhanced expression of VSMC and ECM markers (Figures S1H–S1J). Thus, we elected to use Gen 2 hiPSC-VSMCs-10% FBS ("primed" hiPSC-VSMCs) in subsequent TEVG studies. We routinely attained 181.8 ± 10.3 million VSMCs from ~4.5 million hiPSCs in ~4 weeks, a ~9-fold increase of VSMC yield versus our previous approach (Gui et al., 2016).

We also evaluated the potential of lineage-specific hiPSC-VSMCs for vascular engineering (Cheung et al., 2012). However, lineage-specific hiPSC-VSMCs appeared to be less proliferative than those derived from our EB-based approach (Figure S1K). As tissue engineering requires cells to promptly expand and fill the void space in the scaffolds before the addition of mechanical stimuli, we chose to use EB-derived hiPSC-VSMCs for vascular engineering herein. Future efforts are warranted to obtain lineage specific VSMCs with enhanced proliferative capacity for vessel engineering.

Determination of Culture Medium for hiPSC-TEVGs

Our previous medium for culturing hiPSC-TEVGs contained VSMC lineage-specifying growth factors transforming growth factor β1 (TGF-β1) and platelet-derived growth factor-BB (PDGF-BB) (Gui et al., 2016). However, such medium led to TEVGs with limited mechanical strength. We next investigated the effects of TGF-β1 and PDGF-BB on collagen deposition, cell viability, and preservation of the VSMC phenotype in hiPSC-VSMCs grown on biodegradable PGA scaffolds. The primed hiPSC-VSMCs were seeded onto PGA meshes (5 mm × 5 mm) and cultured in TEVG medium containing TGF-β1 and PDGF-BB (T/P), TGF-β1 only (T/−), PDGF-BB only (−/P), or no growth factor (−/−), respectively, for 3 weeks to form engineered tissues (Figure 2A). Cells effectively populated tissues under all four medium conditions and the tissues cultured in T/P and T/− media appeared to deposit more collagen than those grown in −/P and −/− media (Figures 2B and 2C). A hydroxyproline assay further confirmed that hiPSC-VSMCs produced more collagen per mesh in T/P and T/− media (Figure 2D). T/P and T/− media also appeared to induce higher expression of VSMC markers in hiPSC-VSMCs (Figures 2E and S1L). Moreover, engineered tissues in T/P or −/P medium presented a higher ratio of apoptotic cells (Figures 2F and 2G), suggesting that PDGF-BB may decrease the survival of hiPSC-VSMCs cultured on PGA scaffolds. Thus, a TEVG medium containing TGF-β1 without PDGF-BB (T/−) may provide optimal support for collagen production, cell viability, and maintenance of VSMC properties of hiPSC-VSMCs. In addition, hiPSC-VSMCs in T/− medium readily contracted when exposed to carbachol (Figures S1M and S1N). Based on the above results, we selected to focus on the T/− medium in our vessel engineering studies.

Generation and Characterization of hiPSC-TEVGs

We next investigated the effect of the improved TEVG medium (T/−) on the ECM production and cytoskeletal and metabolic alterations of hiPSC-VSMCs under a workload via mechanical stretching. hiPSC-VSMCs were cultured in the presence of the T/− or T/P medium under static or uniaxial cyclic stretching (2.5% distention at 2.75 Hz) with a FlexCell FX-6000T Tension System. Results suggest that both T/− medium and a 48-h stretching period enhanced the expression of VSMC and ECM markers and the formation of filamentous actin bundles (phalloidin) with a preferred alignment perpendicular to the direction of stretching (Figures S2A–S2C). A hydroxyproline assay further

Figure 2. Optimization of TEVG Medium by Generating Engineered Tissues from Culturing hiPSC-VSMCs on Biodegradable PGA Scaffolds

(A) Schematic illustration for developing tissue patches from primed hiPSC-VSMCs grown on PGA scaffolds.

(B and C) H&E and Masson's trichrome staining of the engineered tissues derived from hiPSC-VSMCs seeded onto PGA scaffold. Red arrowheads indicate PGA remnants. Scale bars, 500 μm.

(D) Collagen weight per mesh of engineered tissue via a hydroxyproline assay.

(E) Immunostaining of the engineered tissues from hiPSC-VSMCs. Sections were stained for the VSMC markers MYH11 and α-SMA. White arrowheads indicate PGA remnants. Scale bar, 100 μm.

(F) TUNEL staining of the engineered tissues from hiPSC-VSMCs. DNA was counterstained by DAPI. White arrowheads indicate the TUNEL-positive apoptotic cells. Scale bar, 100 μm.

(G) Quantification of percentage of TUNEL-positive cells in engineered tissues.

All data are presented as mean ± SEM and were analyzed using a one-way ANOVA with Tukey's multiple comparisons test (n = 3; *p < 0.05; **p < 0.01; N.S, not significant).

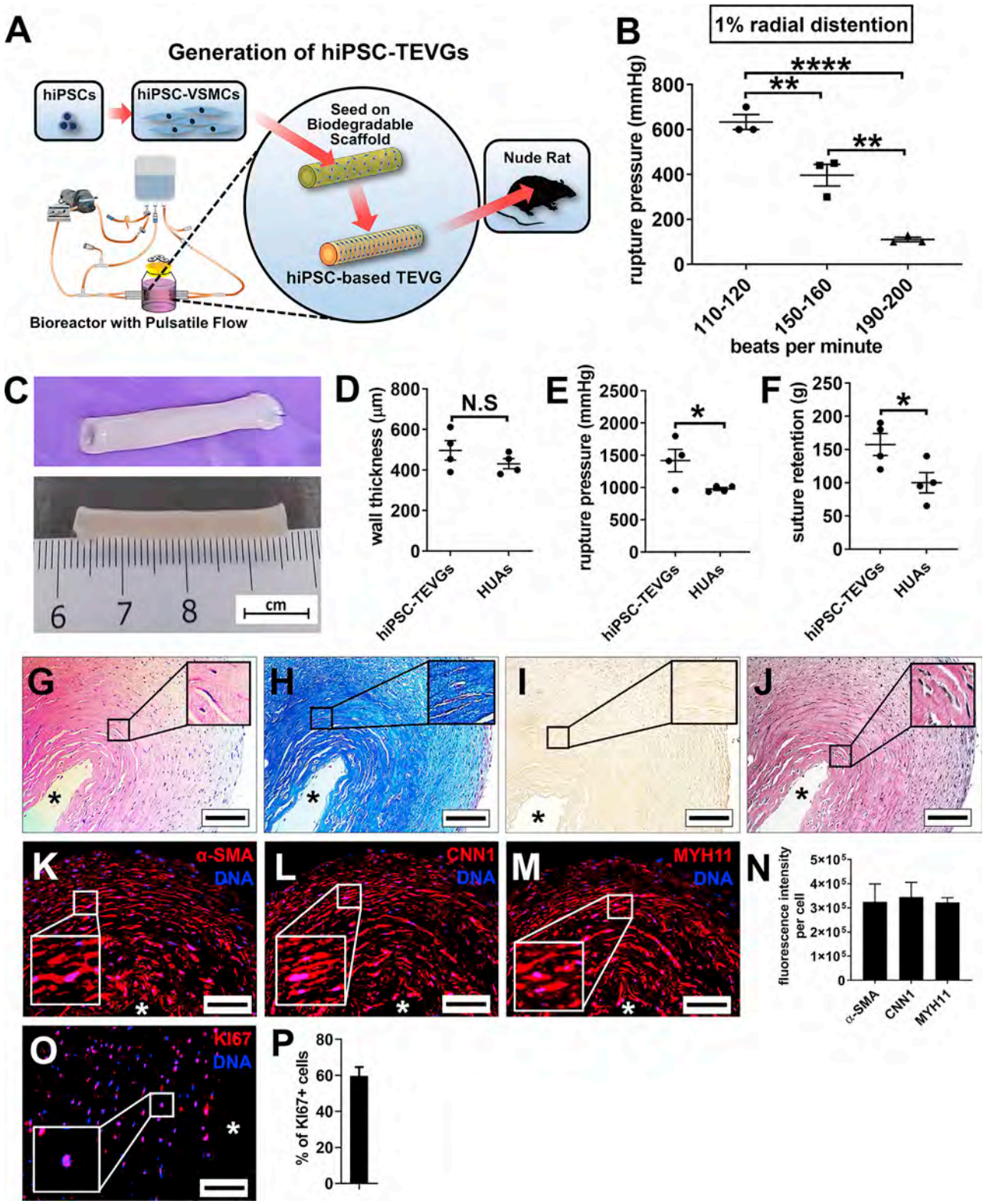

Figure 3. Generation and Characterization of TEVGs from hiPSC-VSMCs under Cyclic Stretch in a Bioreactor with Pulsatile Flow

(A) Schematic illustration for generation and implantation of small caliber (3.2 mm of inner diameter) hiPSC-TEVGs.

(B) The rupture pressures of hiPSC-TEVGs developed after 8 weeks of culture in the presence of pulsatile radial stress with 1% ultimate strain at different rates of 110–120, 150–160, and 190–200 bpm (one-way ANOVA with Tukey's multiple comparisons test). Filled dots, squares, and triangles indicate the values of rupture pressure for individual hiPSC-TEVGs.

(legend continued on next page)

revealed that both T/− medium and stretching promoted collagen deposition in hiPSC-VSMCs (Figure S2D). Moreover, stretching alone increased the expression of focal adhesion (vinculin) or adherens junction (N-cadherin) markers in hiPSC-VSMCs (Figures S2A–S2C).

Mechanical stretching also resulted in an increase in energy production. Since hiPSC-VSMCs were cultured in a TEVG medium based on high-glucose DMEM basal medium (~25 mM glucose), glucose was hypothesized to be the predominant energy source and further investigated. Results showed that stretching increased glucose consumption and cellular ATP production (Figures S2E and S2F). These findings were also reflected transcriptionally with significant upregulation of pivotal glucose-metabolism-associated genes under stretching, including the glucose transporters 1 and 4 (*GLUT1* and *GLUT4*), citrate synthase (*CS*; involved in mitochondrial tricarboxylic acid cycle metabolism), and *PGC1α* (a transcriptional cofactor of mitochondrial biogenesis) (Figure S2A), suggesting a degree of metabolic maturation was induced in these hiPSC-VSMCs. These results suggest that both mechanical stretching and an optimized TEVG medium would potentially promote the generation of hiPSC-based TEVGs with advanced mechanical strength.

We then fabricated TEVGs from hiPSC-VSMCs and augmented their mechanical strength with the inclusion of pulsatile radial stretching. As illustrated in Figure 3A, PGA scaffolds were sewn over silicone tubing (~3.2 mm outer diameter) and connected in bioreactors. Scaffolds were seeded with hiPSC-VSMCs and cultured statically for 1 week. PBS was then flowed by a peristaltic pump into distensible silicone tubing inserted through the vessel lumen, and pulsatile radial stress was applied to the vessels for 7 weeks. Radial stress with 1%–2.5% radial distention (strain) has been applied to develop TEVGs from human primary VSMCs (Dahl et al., 2011; Poh et al., 2005). However, acute addition of 2% strain repeatedly led to the disintegration of the engineered tissue after 3 weeks of culture, suggesting that abrupt exposure to this level of mechanical stress may be detrimental to hiPSC-VSMCs. This phenomenon prompted us to add radial stress incrementally from week 2 to week 4 and then maintain the strain unchanged until the completion of culture. Using this mechanical regimen, hiPSC-TEVGs successfully maintained integrity during the 8-week culture. Previous studies revealed that a pulse rate (bpm) of radial distention at ~165 bpm results in optimal mechanical strength of human or porcine primary VSMC-derived TEVGs (Dahl et al., 2011; Solan et al., 2009). We evaluated the rupture pressure of hiPSC-TEVGs developed in the presence of 1% radial distention at several pulse rates (110–120, 150–160, and 190–200 bpm). Surprisingly, distinct from human primary VSMCs, 110–120 bpm resulted in the highest rupture pressure of hiPSC-TEVGs, and rupture pressure declined dramatically along with an increase in bpm (Figure 3B). Thus, pulsatile radial stress of 110–120 bpm was applied in our hiPSC-TEVGs.

Next, we increased the ultimate strain to 3% and maintained the pulse rate at 110–120 bpm to generate hiPSC-TEVGs. At the end of the 8-week culture period, hiPSC-TEVGs appeared opaque, similar to native vessels (Figure 3C). The wall thickness of hiPSC-TEVGs was 496.8 ± 48.0 μm (Figure 3D). Importantly, hiPSC-TEVGs showed robust mechanical properties indicated by rupture pressure (1419.0 ± 174.4 mmHg) and suture retention strength (157.5 ± 16.5 g) (Figures 3E and 3F) comparable to those of native vessels widely used as coronary artery bypass grafts (saphenous veins, rupture pressure: 1,599 ± 877 mmHg; suture retention strength: 196 ± 29 g) (Dahl et al., 2011). Moreover, the mechanical strength of the hiPSC-TEVGs was markedly higher than that of native human umbilical arteries (HUAs; rupture pressure: 930.4 ± 23.3 mmHg; suture retention strength: 102.5 ± 17.6 g), while the thickness was similar (Figures 3D–3F). In addition, the amount of collagen in hiPSC-TEVGs was 43.1% ± 4.4% (n = 4) of the dry weight of the engineered vessels, which was comparable to that of primary human VSMC-derived TEVGs (31% ± 7%) (Quint et al., 2012) or native blood vessels (HUAs; 36% ± 12%) (Gui et al., 2016). In comparison to the mechanical properties of hiPSC-TEVGs previously developed without pulsatile radial stress (rupture pressure: 500 mmHg; suture retention strength: 30 and 70 g; collagen amount: 12% ± 4% of the dry weight of engineered vessels) (Gui et al., 2016), our current results revealed that the addition of incremental pulsatile radial stretching coupled with the optimized TEVG medium markedly improved the biomechanical properties of hiPSC-TEVGs.

Similar to a human native blood vessel (HUA; Figures S3A–S3J), histological analysis showed hiPSC-TEVGs were highly cellularized (Figure 3G), exhibited robust accretion of collagen (Figure 3H), and lacked obvious calcium deposition (Figure 3I). Similar to previous TEVGs derived from primary or hiPSC-VSMCs (Gui et al., 2016; Niklason et al., 1999), mature ELN fibers were absent in hiPSC-TEVGs (Figure 3J). PGA remnants were seldom observed in hiPSC-TEVGs (Figures 3G–3J), indicating thorough scaffold degradation. Typical VSMC markers were present in the cells within the hiPSC-TEVGs (Figures 3K–3N), similar to those expressed within native HUAs (Figures S3E–S3H). Interestingly, contrary to the minimal number of cells with positivity for the proliferation marker KI67 in native HUAs (Figures S3I and S3J), a significant number of cells in the hiPSC-TEVGs were positive for KI67 (Figures 3O and 3P), potentially due to

(C–F) Generation of hiPSC-TEVGs with 8 weeks of culture in the presence of pulsatile radial stress with 3% ultimate strain at 120 bpm. (C) Representative images of hiPSC-TEVGs after 8 weeks of culture. Scale bar: 1 cm. (D–F) The wall thickness (D), rupture pressure (E), and suture retention strength (F) of hiPSC-TEVGs and native HUAs (two-tailed unpaired Student's t test was performed in D–F; dots indicate the values of results for individual hiPSC-TEVGs or HUAs).

(G–J) Histological examinations (H&E staining, G; Masson's trichrome staining, H; Alizarin red staining, I; and EVG staining, J) of hiPSC-TEVGs were performed. Asterisk indicates the lumen of the graft. Scale bar, 100 μm.

(K–M) Immunostaining of VSMC markers in hiPSC-TEVGs. Sections were stained for α-SMA (K), CNN1 (L), and MYH11 (M). DNA was counterstained by DAPI. Asterisk indicates the lumen of the graft. Scale bar, 100 μm.

(N) Quantification of fluorescence intensity (gray value) of α-SMA, CNN1, and MYH11 per cell from three representative sections (>100 cells/section) in each hiPSC-TEVG.

(O) Immunostaining of KI67 in hiPSC-TEVGs. Asterisk indicates the lumen of the graft. Scale bar, 100 μm.

(P) Quantification of percentage of KI67-positive cells from three representative sections (>100 cells/section) in each hiPSC-TEVG.

All data are presented as mean ± SEM; $n \geq 3$; *$p < 0.05$; **$p < 0.01$; ****$p < 0.0001$; N.S: not significant.

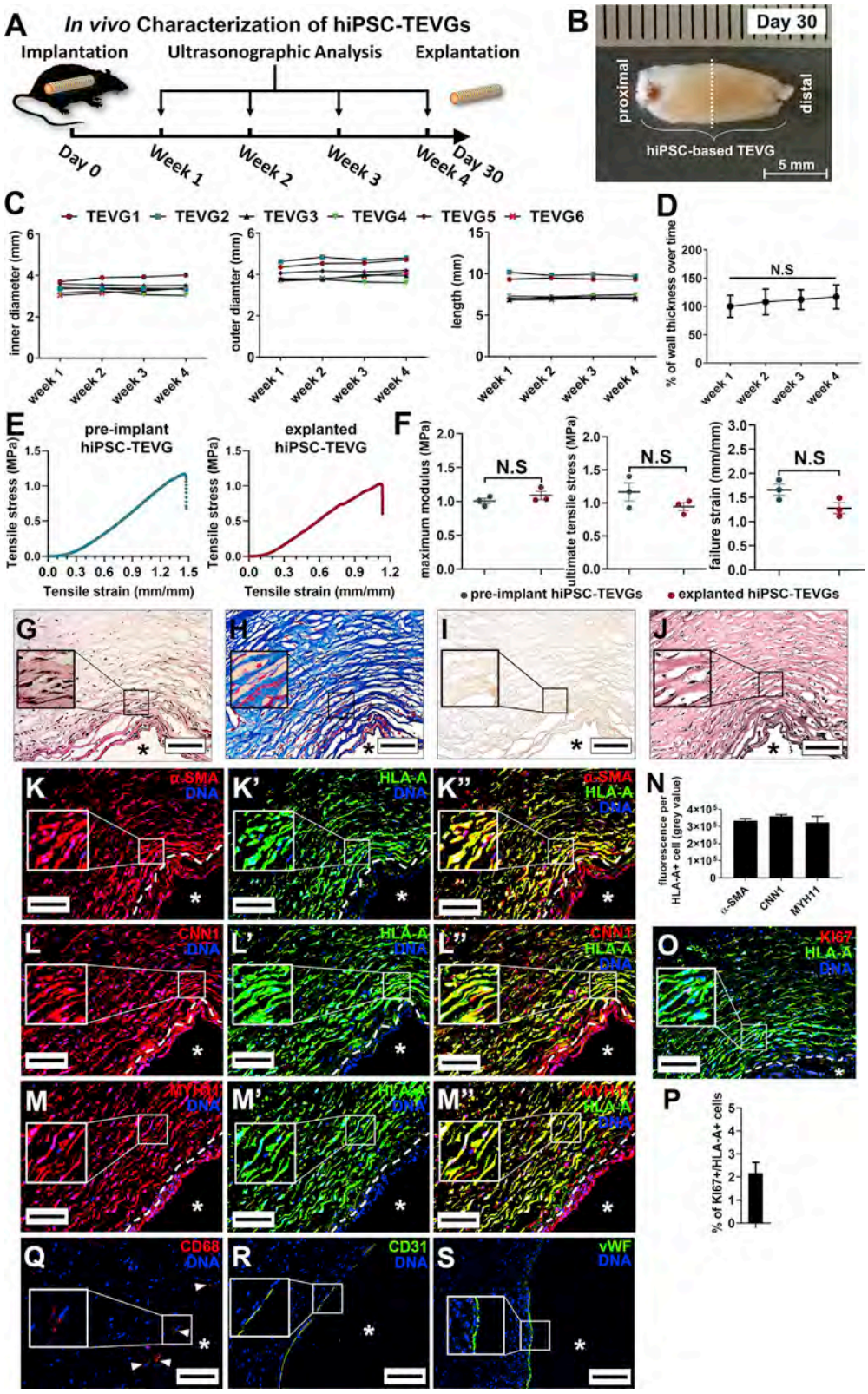

Figure 4. Characterization of hiPSC-TEVGs in Nude Rats 30 Days Post-operation

(A) Schematic illustration for implantation of hiPSC-TEVGs into nude rats and ultrasonographic analysis.

(B) Representative image of explanted TEVG graft (TEVG2) 30 days post-operation. The dashed line indicates the position of sectioning. Scale bar, 5 cm.

(legend continued on next page)

the cell-growth-promoting nature of the TEVG medium. Importantly, cells in hiPSC-TEVGs became largely quiescent under physiological conditions after *in vivo* implantation into the rat abdominal aorta (Figures 4O and 4P). These data suggest that hiPSC-TEVGs displayed the typical histological and cellular phenotypes of engineered vessels.

Implantation of hiPSC-TEVGs into Nude Rats

Six hiPSC-TEVGs were then implanted, as an interpositional graft, into the abdominal aorta of six nude rats (Figure 4A). All rats were followed for 30 days, and the morphometry of implanted hiPSC-TEVGs (mid-graft inner diameter, mid-graft outer diameter, and length) were assessed weekly via ultrasonography (Figure 4A). All implanted grafts were patent when harvested, and no sign of rupture or aberrant deformation was observed in any of the explants (Figure 4B), potentially due to the high mechanical strength of the grafts (Figures 3E and 3F). No sign of teratoma formation was observed in any animals. Ultrasonography revealed that the grafts did not present any evident dilation, elongation, or wall thickening (Figures 4C and 4D). Limited thrombosis was observed at distal ends of some TEVGs, possibly due to the lack of an endothelial lining prior to graft implantation in this proof-of-principle study and/or the potential intraluminal turbulence of blood flow. These results indicated that the hiPSC-TEVGs were able to withstand aortic blood pressure during the period of evaluation.

Next, we examined the mechanical properties of the explanted hiPSC-TEVGs by cutting them into tissue rings and deriving stress-strain plots. As a reference, tissue rings made from the same hiPSC-TEVG prior to implantation were also measured for comparison. The mechanical properties, including maximum modulus, ultimate tensile stress, and failure strain of tissue rings derived from hiPSC-TEVGs pre- and post-implantation, appeared to be statistically comparable (Figures 4E and 4F). Tissue rings derived from native porcine coronary arteries were used as a control (Figure S3K). The porcine arterial rings showed a higher failure strain and a trend toward an enhanced ultimate tensile stress and a reduced maximum modulus compared with the hiPSC-TEVG counterparts (Figures S3L–S3O), potentially due to more effective ELN and collagen deposition in the native porcine vessels. We also evaluated the contractile function of the tissue rings sectioned from hiPSC-TEVGs in the presence of the vasoconstrictor carbachol (Figure S3P). No statistically significant difference was detected between the contractility of pre-implant and explanted hiPSC-TEVGs (Figure S3Q). There appeared to be a trend of decreased contractility in the explanted tissue rings ($p = 0.13$), possibly due to suboptimal luminal lining and remodeling. In summary, these results suggest that hiPSC-TEVGs maintained mechanical strength and contractile function after implantation.

Histological analysis revealed that explanted grafts remained cellularized (Figure 4G), that extracellular collagen was abundantly deposited (Figure 4H), and there was no apparent calcification in the media of the grafts (Figure 4I). Mature ELN fibers were not detected (Figure 4J), similar to previously reported TEVGs derived from hiPSC-VSMCs or primary VSMCs (Gui et al., 2016; Niklason et al., 1999). VSMC markers were readily observed in human cells (positive for human HLA-A staining, above the white dashed line in Figures 4K–4M and S3R) within the grafts and were expressed in hiPSC-VSMCs in explanted TEVGs (Figure 4N) at levels comparable to hiPSC-VSMCs in pre-implant grafts (Figure 3N). A minimal number of human cells in the grafts were positive for the proliferation marker KI67 (Figures 4O and 4P), suggesting that hiPSC-derived cells within the vessel walls were primarily in a quiescent state, which was similar to cells in the human native HUAs (Figures S3I and S3J). In addition, only very limited numbers of $CD68^+$ cells were observed near the luminal side, suggesting minimal or no presence of macrophages in the grafts (Figure 4Q). Notably, some portions of the luminal surface displayed coverage by endothelial cells from the host, revealed by CD31 and von Willebrand factor (vWF) staining (Figures 4R and 4S). In summary, these data suggest that hiPSC-derived cells in the engineered vessel preserved their mature VSMC phenotype following *in vivo* implantation.

DISCUSSION

The current study represents the most mechanically robust derivation of TEVGs from hiPSC-VSMCs in the field, with properties approaching those of native vessels used for arterial bypass. This advancement is based on a routine production (~180 million) of functional VSMCs from self-renewable hiPSCs, an optimized TEVG culture medium, and a beneficial biophysical training regimen of hiPSC-TEVGs in a bioreactor. Importantly,

(C) The inner diameters, outer diameters, and length of the six implanted hiPSC-TEVGs over time during 30 days of implantation by ultrasonographic analysis.
(D) Wall thickness of six hiPSC-TEVGs during 30 days of implantation by ultrasonographic analysis (one-way ANOVA with Tukey's multiple comparisons test). Note that wall thickness of each TEVG during the 4-week implantation was normalized to the average wall thickness of TEVGs 1 week post-implantation.
(E) Representative stress-strain plots of tissue rings sectioned from pre-implant or explanted hiPSC-TEVGs.
(F) Mechanical parameters (maximum modulus, ultimate tensile stress, and failure strain) were compared between the tissue rings sectioned from pre-implant or explanted hiPSC-TEVGs (two-tailed paired Student's t test).
(G–J) Histological analysis (H&E staining, G; Masson's trichrome staining, H; Alizarin red staining, I; and EVG staining, J) of explanted hiPSC-TEVGs (TEVG2). Scale bar: 100 μm.
(K–S) Immunostaining of sections of hiPSC-TEVGs. The sections were stained for the VSMC markers α-SMA (K, K′, and K″), CNN1 (L, L′, and L″), and MYH11 (M, M′, and M″), and fluorescence intensity (gray value) of α-SMA, CNN1, and MYH11 per HLA-A-positive cell from three representative sections (>80 cells/section) in each hiPSC-TEVG was quantified (N). The cell proliferation marker KI67 was stained (O), and the percentage of KI67-positive cells in HLA-A-positive cells (>80 cells/section) in each hiPSC-TEVG was quantified (P). Additionally, sections were stained for the macrophage marker CD68 (Q) (positive cells indicated by white arrowheads) and the endothelial cell markers CD31 (R) and vWF (S). The human-specific surface antigen (HLA-A) was stained to indicate the human cells in TEVGs (K–M). The white dashed line indicates the boundary between the human cells and host rat cells (K–M and O). DNA was counterstained by DAPI. Asterisks indicate the lumen of the graft. Scale bar, 100 μm.
All data are presented as mean ± SEM ($n \geq 3$; N.S, not significant).

hiPSC-TEVGs showed excellent patency without radial dilation or longitudinal elongation and effectively maintained both mechanical and contractile function 4 weeks after aortic implantation in rats. This study has thus established the foundation for large-scale manufacture of mechanically robust hiPSC-TEVGs as an efficacious therapy (Figures 1B and 1C).

Additionally, this technology could integrate immunocompatible, HLA-engineered universal hiPSC lines (Deuse et al., 2019; Gornalusse et al., 2017; Xu et al., 2019) in the future for allogeneic graft implantation as a treatment option for any patient in need (Figure 1B). We derived VSMCs from hiPSCs with enhanced immunocompatibility, in which both HLA-A and HLA-B alleles and HLA class II are disrupted (Figure S4A; Xu et al., 2019). Such hiPSC-VSMCs expressed VSMC and ECM markers (Figure S4B), showed contraction in response to carbachol (Figures S4C and S4D), and formed vascular tissue on PGA scaffolds with effective collagen production (Figures S4E–S4J), suggesting the potential feasibility of vascular tissue engineering using HLA-edited, immunocompatible hiPSCs.

There are limitations and challenges remaining to be addressed in this study. The mechanisms by which TGF-β1 modulates the expression of VSMC and glucose metabolism markers via the SMAD-dependent or SMAD-independent pathway in conjunction with myocardin/myocardin-related transcription factor (MRTF)/serum response factor (SRF) signaling (Bernard et al., 2015; Shi and Chen, 2016), as well as the correlation between metabolic activity and cellular contractility in hiPSC-VSMCs, awaits in-depth investigation. Future endeavors will also be made to understand how removal of FGF2 and EGF in the primed medium may relieve their antagonizing effect on TGF-β1 in regulation of VSMC marker expression.

In addition, similar to previously engineered vessels (Dahl et al., 2011; Niklason et al., 1999), hiPSC-TEVGs did not contain mature ELN fibers, expected to be imperative for an effective treatment for patients with peripheral and coronary arterial diseases. In a longer-term *in vivo*, 60-day rat aortic implantation of hiPSC-TEVGs, although mature ELN fibers were not observed in the medial layers, limited extracellular, discontinuous ELN fibers were detected via elastic Verhoeff-Van Gieson (EVG) staining (green arrows in Figure S4O). Future endeavors are warranted to perform long-term hiPSC-TEVG implantation for ELN detection. It has been shown that hiPSC-VSMCs seeded onto 3D electrospun scaffolds in a quiescent medium containing 0.5% FBS and 1 ng/ml TGF-β1 under laminar shear stress resulted in promising ELN fiber formation (Eoh et al., 2017). Further optimization is warranted to develop an optimized medium with balanced cell proliferation and ELN deposition. ELN expression in hiPSC-TEVGs could be enhanced by retinoic acid, insulin-like growth factor-1, or a nitric oxide donor (Sugitani et al., 2001; Watson et al., 2008; Wolfe et al., 1993). Moreover, ELN assembly could be reinforced through the treatment of BMP4 or LTBP4 via enhancing the deposition of essential ECM proteins that interact with and stabilize ELN (Noda et al., 2013; Tojais et al., 2017). In addition, enhancement of ELN cross-linking could be achieved by augmenting lysyl oxidase function (Smith-Mungo and Kagan, 1998; Sugitani et al., 2001).

To further enhance the biomechanical strength of hiPSC-TEVGs to approach that of the human internal thoracic artery (rupture pressure: 3,196 ± 1,264 mmHg; suture retention: 138 ± 50 g) (Dahl et al., 2011), optimization of pulsatile stretching from current 3% strain up to 5% will be explored. Moreover, oxygenation of the TEVG medium will be enhanced to promote cellular growth and ECM production. Additionally, endothelialization of hiPSC-TEVGs is needed to enhance their vascular function in future endeavors. In summary, the derivation of hiPSC-TEVGs with robust mechanical strength in this study will move the vessel-engineering field forward and set the stage for innovative therapies for patients with cardiovascular diseases.

STAR★METHODS

Detailed methods are provided in the online version of this paper and include the following:

- KEY RESOURCES TABLE
- LEAD CONTACT AND MATERIALS AVAILABILITY
- EXPERIMENTAL MODEL AND SUBJECT DETAILS
  - Wild-type Human Induced Pluripotent Stem Cells
  - HLA-C-retained (CIITA-knockout) Human Induced Pluripotent Stem Cells
  - Human Vascular Smooth Muscle Cells
  - Human Umbilical Vein Endothelial Cells
  - Animal Use
  - Human Umbilical Arteries
  - Porcine Coronary Arteries
- METHOD DETAILS
  - Generation of VSMCs from hiPSCs
  - Immunostaining of Cultured Cells
  - Quantitative Reverse Transcription PCR
  - Cell Contractility Assay
  - MTT Assay
  - Culturing hiPSC-VSMCs on 5 mm x 5 mm PGA Scaffolds
  - Tissue Immunohistochemistry and Histology
  - TUNEL Assay
  - Hydroxyproline Assay
  - Cell Culture with Pulsatile Uniaxial Stretch
  - Evaluation of Glucose in Media
  - Evaluation of Cellular ATP Concentration
  - Generation of hiPSC-TEVGs
  - Implantation of hiPSC-TEVG into Nude Rat
  - Ultrasonographical Assessment of Grafts
  - Mechanical Evaluation of hiPSC-TEVGs
  - Contractility Evaluation of hiPSC-TEVGs
- QUANTIFICATION AND STATISTICAL ANALYSES
- DATA AND CODE AVAILABILITY

SUPPLEMENTAL INFORMATION

Supplemental Information can be found online at https://doi.org/10.1016/j.stem.2019.12.012.

ACKNOWLEDGMENTS

This work was supported by NIH (United States) grant 1R01HL116705 and CRMRF (United States) grants 12-SCB-YALE-06 and 15-RMB-YALE-08 (Y.Q.). This work was also supported by AHA (United States) grant 19POST34450100 (J.L.) and NIH (United States) grants F31-HL143924 and

T32-GM0007324 (M.W.E.). We thank Christopher Anderson, Luke Batty, Tristan Driscoll, and Minghao Chen for their support.

AUTHOR CONTRIBUTIONS

Y.Q., J.L., L.G., L.E.N., A.D., G.T., and S.C. conceived the study; J.L., L.Q., L.Z., L.G., M.H.K., Y.H., M.W.E., J.A.C., S.O., J.W., Y.Y., S.-M.Z., X.C., and G.L. performed research; J.L., L.Q., L.G., M.H.K., Y.H., M.W.E., J.A.C., S.O., J.W., Y.Y., S.-M.Z., L.E.N., and Y.Q. analyzed data; J.L. and Y.Q. wrote the manuscript; and J.L., M.W.E., M.R., C.L., Y.H., L.E.N., and Y.Q. edited the manuscript.

DECLARATION OF INTERESTS

L.E.N. is a founder and shareholder in Humacyte. Humacyte produces engineered blood vessels from allogeneic smooth muscle cells for vascular surgery. L.E.N.'s spouse has equity in Humacyte, and L.E.N. serves on Humacyte's Board of Directors. L.E.N. is an inventor on patents that are licensed to Humacyte and produce royalties for L.E.N. Humacyte neither funded current studies nor influenced the conduct, description, or interpretation of the findings in this report. The authors declare a patent filed related to this work.

Received: February 1, 2019
Revised: October 25, 2019
Accepted: December 23, 2019
Published: January 16, 2020

REFERENCES

Akoh, J.A., and Patel, N. (2010). Infection of hemodialysis arteriovenous grafts. J. Vasc. Access *11*, 155–158.

Atchison, L., Zhang, H., Cao, K., and Truskey, G.A. (2017). A tissue engineered blood vessel model of Hutchinson-Gilford progeria syndrome using human iPSC-derived smooth muscle cells. Sci. Rep. *7*, 8168.

Bajpai, V.K., Mistriotis, P., Loh, Y.H., Daley, G.Q., and Andreadis, S.T. (2012). Functional vascular smooth muscle cells derived from human induced pluripotent stem cells via mesenchymal stem cell intermediates. Cardiovasc. Res. *96*, 391–400.

Bernard, K., Logsdon, N.J., Ravi, S., Xie, N., Persons, B.P., Rangarajan, S., Zmijewski, J.W., Mitra, K., Liu, G., Darley-Usmar, V.M., and Thannickal, V.J. (2015). Metabolic reprogramming is required for myofibroblast contractility and differentiation. J. Biol. Chem. *290*, 25427–25438.

Chen, P.Y., Qin, L., Li, G., Tellides, G., and Simons, M. (2016). Fibroblast growth factor (FGF) signaling regulates transforming growth factor beta (TGFβ)-dependent smooth muscle cell phenotype modulation. Sci. Rep. *6*, 33407.

Cheung, C., Bernardo, A.S., Trotter, M.W., Pedersen, R.A., and Sinha, S. (2012). Generation of human vascular smooth muscle subtypes provides insight into embryological origin-dependent disease susceptibility. Nat. Biotechnol. *30*, 165–173.

Conte, M.S. (2013). Critical appraisal of surgical revascularization for critical limb ischemia. J. Vasc. Surg. *57* (2, Suppl), 8S–13S.

Dahl, S.L., Kypson, A.P., Lawson, J.H., Blum, J.L., Strader, J.T., Li, Y., Manson, R.J., Tente, W.E., DiBernardo, L., Hensley, M.T., et al. (2011). Readily available tissue-engineered vascular grafts. Sci. Transl. Med. *3*, 68ra9.

Dash, B.C., Levi, K., Schwan, J., Luo, J., Bartulos, O., Wu, H., Qiu, C., Yi, T., Ren, Y., Campbell, S., et al. (2016). Tissue-engineered vascular rings from human iPSC-derived smooth muscle cells. Stem Cell Reports *7*, 19–28.

Deuse, T., Hu, X., Gravina, A., Wang, D., Tediashvili, G., De, C., Thayer, W.O., Wahl, A., Garcia, J.V., Reichenspurner, H., et al. (2019). Hypoimmunogenic derivatives of induced pluripotent stem cells evade immune rejection in fully immunocompetent allogeneic recipients. Nat. Biotechnol. *37*, 252–258.

Dijkman, P.E., Driessen-Mol, A., Frese, L., Hoerstrup, S.P., and Baaijens, F.P. (2012). Decellularized homologous tissue-engineered heart valves as off-the-shelf alternatives to xeno- and homografts. Biomaterials *33*, 4545–4554.

Elliott, M.B., Ginn, B., Fukunishi, T., Bedja, D., Suresh, A., Chen, T., Inoue, T., Dietz, H.C., Santhanam, L., Mao, H.Q., et al. (2019). Regenerative and durable small-diameter graft as an arterial conduit. Proc. Natl. Acad. Sci. USA *116*, 12710–12719.

Eoh, J.H., Shen, N., Burke, J.A., Hinderer, S., Xia, Z., Schenke-Layland, K., and Gerecht, S. (2017). Enhanced elastin synthesis and maturation in human vascular smooth muscle tissue derived from induced-pluripotent stem cells. Acta Biomater. *52*, 49–59.

Gornalusse, G.G., Hirata, R.K., Funk, S.E., Riolobos, L., Lopes, V.S., Manske, G., Prunkard, D., Colunga, A.G., Hanafi, L.A., Clegg, D.O., et al. (2017). HLA-E-expressing pluripotent stem cells escape allogeneic responses and lysis by NK cells. Nat. Biotechnol. *35*, 765–772.

Gui, L., Dash, B.C., Luo, J., Qin, L., Zhao, L., Yamamoto, K., Hashimoto, T., Wu, H., Dardik, A., Tellides, G., et al. (2016). Implantable tissue-engineered blood vessels from human induced pluripotent stem cells. Biomaterials *102*, 120–129.

Kim, B.S., Nikolovski, J., Bonadio, J., and Mooney, D.J. (1999). Cyclic mechanical strain regulates the development of engineered smooth muscle tissue. Nat. Biotechnol. *17*, 979–983.

Lawson, J.H., Glickman, M.H., Ilzecki, M., Jakimowicz, T., Jaroszynski, A., Peden, E.K., Pilgrim, A.J., Prichard, H.L., Guziewicz, M., Przywara, S., et al. (2016). Bioengineered human acellular vessels for dialysis access in patients with end-stage renal disease: two phase 2 single-arm trials. Lancet *387*, 2026–2034.

Luo, J., Qin, L., Kural, M.H., Schwan, J., Li, X., Bartulos, O., Cong, X.Q., Ren, Y., Gui, L., Li, G., et al. (2017). Vascular smooth muscle cells derived from inbred swine induced pluripotent stem cells for vascular tissue engineering. Biomaterials *147*, 116–132.

Madden, R.L., Lipkowitz, G.S., Browne, B.J., and Kurbanov, A. (2005). A comparison of cryopreserved vein allografts and prosthetic grafts for hemodialysis access. Ann. Vasc. Surg. *19*, 686–691.

McAllister, T.N., Maruszewski, M., Garrido, S.A., Wystrychowski, W., Dusserre, N., Marini, A., Zagalski, K., Fiorillo, A., Avila, H., Manglano, X., et al. (2009). Effectiveness of haemodialysis access with an autologous tissue-engineered vascular graft: a multicentre cohort study. Lancet *373*, 1440–1446.

Niklason, L.E., Gao, J., Abbott, W.M., Hirschi, K.K., Houser, S., Marini, R., and Langer, R. (1999). Functional arteries grown in vitro. Science *284*, 489–493.

Noda, K., Dabovic, B., Takagi, K., Inoue, T., Horiguchi, M., Hirai, M., Fujikawa, Y., Akama, T.O., Kusumoto, K., Zilberberg, L., et al. (2013). Latent TGF-β binding protein 4 promotes elastic fiber assembly by interacting with fibulin-5. Proc. Natl. Acad. Sci. USA *110*, 2852–2857.

Patsch, C., Challet-Meylan, L., Thoma, E.C., Urich, E., Heckel, T., O'Sullivan, J.F., Grainger, S.J., Kapp, F.G., Sun, L., Christensen, K., et al. (2015). Generation of vascular endothelial and smooth muscle cells from human pluripotent stem cells. Nat. Cell Biol. *17*, 994–1003.

Piez, K., and Likins, R.C. (1960). The nature of collagen. In Calcification in Biological Systems: A Symposium Presented at the Washington Meeting of the American Association for the Advancement of Science, December 29, 1958, R.F. Sognnaes, ed. (American Association for the Advancement of Science), pp. 411–420.

Poh, M., Boyer, M., Solan, A., Dahl, S.L., Pedrotty, D., Banik, S.S., McKee, J.A., Klinger, R.Y., Counter, C.M., and Niklason, L.E. (2005). Blood vessels engineered from human cells. Lancet *365*, 2122–2124.

Quint, C., Arief, M., Muto, A., Dardik, A., and Niklason, L.E. (2012). Allogeneic human tissue-engineered blood vessel. J. Vasc. Surg. *55*, 790–798.

Schlumberger, W., Thie, M., Rauterberg, J., and Robenek, H. (1991). Collagen synthesis in cultured aortic smooth muscle cells. Modulation by collagen lattice culture, transforming growth factor-beta 1, and epidermal growth factor. Arterioscler. Thromb. *11*, 1660–1666.

Shi, N., and Chen, S.Y. (2016). Smooth muscle cell differentiation: model systems, regulatory mechanisms, and vascular diseases. J. Cell. Physiol. *231*, 777–787.

Smith-Mungo, L.I., and Kagan, H.M. (1998). Lysyl oxidase: properties, regulation and multiple functions in biology. Matrix Biol. *16*, 387–398.

Solan, A., Dahl, S.L., and Niklason, L.E. (2009). Effects of mechanical stretch on collagen and cross-linking in engineered blood vessels. Cell Transplant. *18*, 915–921.

Song, H.G., Rumma, R.T., Ozaki, C.K., Edelman, E.R., and Chen, C.S. (2018). Vascular tissue engineering: progress, challenges, and clinical promise. Cell Stem Cell *22*, 340–354.

Spinetti, G., Kraenkel, N., Emanueli, C., and Madeddu, P. (2008). Diabetes and vessel wall remodelling: from mechanistic insights to regenerative therapies. Cardiovasc. Res. *78*, 265–273.

Sugitani, H., Wachi, H., Tajima, S., and Seyama, Y. (2001). Nitric oxide stimulates elastin expression in chick aortic smooth muscle cells. Biol. Pharm. Bull. *24*, 461–464.

Syedain, Z.H., Graham, M.L., Dunn, T.B., O'Brien, T., Johnson, S.L., Schumacher, R.J., and Tranquillo, R.T. (2017). A completely biological "off-the-shelf" arteriovenous graft that recellularizes in baboons. Sci. Transl. Med. *9*, eaan4209.

Takahashi, K., Tanabe, K., Ohnuki, M., Narita, M., Ichisaka, T., Tomoda, K., and Yamanaka, S. (2007). Induction of pluripotent stem cells from adult human fibroblasts by defined factors. Cell *131*, 861–872.

Tojais, N.F., Cao, A., Lai, Y.J., Wang, L., Chen, P.I., Alcazar, M.A.A., de Jesus Perez, V.A., Hopper, R.K., Rhodes, C.J., Bill, M.A., et al. (2017). Codependence of bone morphogenetic protein receptor 2 and transforming growth factor-β in elastic fiber assembly and its perturbation in pulmonary arterial hypertension. Arterioscler. Thromb. Vasc. Biol. *37*, 1559–1569.

Wang, Y., Hu, J., Jiao, J., Liu, Z., Zhou, Z., Zhao, C., Chang, L.J., Chen, Y.E., Ma, P.X., and Yang, B. (2014). Engineering vascular tissue with functional smooth muscle cells derived from human iPS cells and nanofibrous scaffolds. Biomaterials *35*, 8960–8969.

Watson, R.E., Long, S.P., Bowden, J.J., Bastrilles, J.Y., Barton, S.P., and Griffiths, C.E. (2008). Repair of photoaged dermal matrix by topical application of a cosmetic 'antiageing' product. Br. J. Dermatol. *158*, 472–477.

Wolfe, B.L., Rich, C.B., Goud, H.D., Terpstra, A.J., Bashir, M., Rosenbloom, J., Sonenshein, G.E., and Foster, J.A. (1993). Insulin-like growth factor-I regulates transcription of the elastin gene. J. Biol. Chem. *268*, 12418–12426.

Wu, W., Allen, R.A., and Wang, Y. (2012). Fast-degrading elastomer enables rapid remodeling of a cell-free synthetic graft into a neoartery. Nat. Med. *18*, 1148–1153.

Xu, H., Wang, B., Ono, M., Kagita, A., Fujii, K., Sasakawa, N., Ueda, T., Gee, P., Nishikawa, M., Nomura, M., et al. (2019). Targeted disruption of HLA genes via CRISPR-Cas9 generates iPSCs with enhanced immune compatibility. Cell Stem Cell *24*, 566–578.e567.

STAR★METHODS

KEY RESOURCES TABLE

REAGENT or RESOURCE	SOURCE	IDENTIFIER
Antibodies		
α-SMA	Sigma	Cat# A5228; RRID: AB_262054
CNN1	Sigma	Cat# C2687; RRID: AB_476840
MYH11	Abcam	Cat# ab53219; RRID: AB_2147146
COL1	Abcam	Cat# ab34710; RRID: AB_731684
ELN	Abcam	Cat# ab21610; RRID: AB_446423
OCT4	Abcam	Cat# ab18976; RRID: AB_444714
N-cadherin	Santa Cruz	Cat# sc-7939; RRID: AB_647794
HLA-A	Abcam	Cat# ab52922; RRID: AB_881225
HLA-A	Santa Cruz	Cat# sc-365485; RRID: AB_10859213
KI67	BD bioscience	Cat# 550609; RRID: AB_393778
CD31	Abcam	Cat# ab28364; RRID: AB_726362
CD68	Abcam	Cat# ab31630; RRID: AB_1141557
vWF	Santa Cruz	Cat# sc-8068; RRID: AB_2216590
Alexa 488 goat anti-mouse IgG	ThermoFisher	Cat# A-11029; RRID: AB_138404
Alexa 488 goat anti-rabbit IgG	ThermoFisher	Cat# A-11008; RRID: AB_143165
Alexa 555 goat anti-mouse IgG	ThermoFisher	Cat# A21426; RRID: AB_1500929
Alexa 555 goat anti-rabbit IgG	ThermoFisher	Cat# A-21428; RRID: AB_141784
Alexa 647 goat anti-mouse IgG	ThermoFisher	Cat# A-21235; RRID: AB_2535804
Alexa 647 goat anti-rabbit IgG	ThermoFisher	Cat# A-21245; RRID: AB_141775
Alexa 488 donkey anti-goat IgG	ThermoFisher	Cat# A-11055; RRID: AB_2534102
Biological Samples		
human umbilical cord arteries	Yale–New Haven Hospital	N/A
porcine coronary arteries	Yale University, Veterinary Clinical Services	N/A
Chemicals, Peptides, and Recombinant Proteins		
mTeSR1 medium kit	STEMCELL Technology	85850
Ethylenediaminetetraacetic acid (EDTA)	ThermoFisher	15575020
Dispase II	ThermoFisher	17105041
Matrigel, growth factor reduced	BD Corning	354230
Y-27632	Millipore	1254
Dulbecco's Modified Eagle Medium	ThermoFisher	11965-092
Fetal bovine serum	Gemini	100-106
L-glutamine	ThermoFisher	25030-081
Non-essential amino acid	ThermoFisher	11140-050
Penicillin/streptomycin	ThermoFisher	15140-122
β-mercaptoethanol	Sigma-Aldrich	M3148-25ml
0.05% trypsin-EDTA	ThermoFisher	25300-054
Sodium pyruvate	ThermoFisher	11360-070
Recombinant human TGFβ1	Peprotech	100-21C-10UG
Recombinant human PDGF-BB	Peprotech	220-BB-050
Ham's F-12 nutrient mix	ThermoFisher	11765054
Iscove's Modified Dulbecco's Medium (IMDM)	ThermoFisher	12440053
Chemically-defined lipid concentrate	ThermoFisher	11905031

(*Continued on next page*)

Continued

REAGENT or RESOURCE	SOURCE	IDENTIFIER
Monothioglycerol	Sigma-Aldrich	M6145
Transferrin	Roche	652202
Insulin (for lineage-specific VSMC differentiation)	Roche	1376497
Poly(vinyl alcohol)	Sigma-Aldrich	P8136
Recombinant human BMP4	R&D System	314-BP
Recombinant human FGF2	R&D System	233-FB
LY294002	Sigma-Aldrich	L9908
SB431542	Sigma-Aldrich	S4317
Gelatin	ThermoFisher	G2500-100G
Smooth Muscle Growth Medium-2 (SmGM) Bullet Kit	Lonza	CC-3182
Endothelial Cell Growth Medium-2 (EGM-2) Bullet Kit	Lonza	CC-3162
Normal goat serum	ThermoFisher	10000C
Dulbecco's Phosphate-Buffered Saline	ThermoFisher	14190-144
Triton X-100	AmericanBIO	AB02025-00500
4,6-diamidino-2-phenylindole (DAPI)	ThermoFisher	D1306
Alexa Fluor 568 Phalloidin	ThermoFisher	A12380
Carbachol	Abcam	ab141354
3-(4,5-dimethylthiazol-2-yl)-2,5-diphenyl tetrazolium bromide (MTT)	Sigma-Aldrich	M2128
Nonwoven-PGA polymer mesh, 1.0 mmx5-6 mg/cm^2, 20cmx30cm	BIOFELT	N/A
Sodium hydroxide	Sigma-Aldrich	S0899
Ascorbic acid	Sigma-Aldrich	A4544-25 g
Proline	Sigma-Aldrich	P5607-25 g
Glycine	Sigma-Aldrich	G8790-100 g
Alanine	Sigma-Aldrich	A7469-25 g
CuSO4	Sigma-Aldrich	C8027-500G
Penicillin G	Sigma-Aldrich	PENNA-1MU
Human recombinant insulin (for TEVG culture)	Sigma-Aldrich	I9080-50mg
Sodium chloride	Sigma-Aldrich	S9625
Potassium chloride	Sigma-Aldrich	P5405
Magnesium chloride	Sigma-Aldrich	M8266
HEPES	Sigma-Aldrich	H3375
Dextrose	Sigma-Aldrich	D9434
Calcium chloride dihydrate	Sigma-Aldrich	C7902
Sucrose	Sigma-Aldrich	S3089-1kg
Tissue-Tek O.C.T. Compound	Sakura Finetek	4583
Ultra-pure agarose	Sigma-Aldrich	16500-500
Critical Commercial Assays		
TRIzol RNA Isolation Kit	ThermoFisher	15596108
iScript cDNA synthesis Kit	BIO-RAD	170-8891
iQ SYBR Green Supermix	BIO-RAD	1708882
Hydroxyproline assay kit	Sigma-Aldrich	MAK008
TUNEL staining kit	Roche	11684795910
ATP Assay Kit (Colorimetric)	Abcam	ab83355
Experimental Models: Cell Lines		
Y6 human induced pluripotent stem cells	Yale University, Stem Cell Research Center	N/A
HLA-C retained (CIITA) human induced pluripotent stem cells (585A1-C7-only#3-1+CIITA-ex3g5-NF #6)	Center for iPS Cell Research and Application (CiRA), Kyoto University	N/A

(*Continued on next page*)

Continued

REAGENT or RESOURCE	SOURCE	IDENTIFIER
Primary human aortic smooth muscle cells	Lonza	cc-2571
Human umbilical vein endothelial cells	Lonza	cc-2517
Experimental Models: Organisms/Strains		
NIH-Foxn1rnu nude rats (10-week-old, male, 300 g)	Charles River	NIH-Foxn1rnu nude rats
Oligonucleotides		
qRT-PCR primers	This paper	Table S1
Software and Algorithms		
ImageJ	National Institutes of Health	https://imagej.nih.gov/ij/
GraphPad Prism 8	GraphPad Software	https://www.graphpad.com/
Other		
Costar® Ultra-Low Attachment 6 Well Plate	Corning	3471
Costar® Ultra-Low Attachment 24 Well Plate	Corning	3473
UniFlex® Culture Plates	Flexcell® International Corporation	UF-4001U-Each
FX-6000T Tension System	Flexcell® International Corporation	N/A
Glass bioreactors for TEVG culture	Yale University, Scientific Glassblowing Laboratory	N/A
Cole-Parmer PTFE Syringe Filters, Sterile; 0.20 μm, 25 mm Diameter (Air filter of TEVG bioreactor)	Cole-Parmer	EW-02915-08
Masterflex Replacement controller for 07553-series L/S systems, 115V (peristaltic pump for TEVG culture)	Cole-Parmer	EW-07553-71
Masterflex L/S Easy-Load® II Head for Precision Tubing, PPS/SS (Head of peristaltic pump)	Cole-Parmer	EW-77200-60
Masterflex L/S PharMed BPT Tubing, L/S #18, 25 ft (connection tubing for bioreactor, large)	Cole-Parmer	EW-06508-18
Masterflex L/S PharMed BPT Tubing, L/S #16 (connection tubing for bioreactor, small)	Cole-Parmer	EW-06508-16
Masterflex L/S BioPharm Platinum-Cured Silicone Pump Tubing, L/S 16 (feeding tubing)	Cole-Parmer	EW-96420-16
4-0 Surgipro blue 36" cv-25 taper, double armed (surgical suture to stitch PGA scaffold to the Dacron arm)	Medtronic Animal Health	VP761X
Coated Vicryl® (polyglactin 910) suture (surgical suture to sew the tubule PGA scaffold around the silicon tube)	Ethicon	J492G
HEMASHIELD PLATINUM Woven Double Velour Vascular Grafts (Dacron to anchor the PGA scaffold to the glass arm)	Maquet	175438P
Silicon tube (inner diameter 3.2 mm)	Saint-Gobain	F05027
Edward Truwave DPT Px600f Pressure Monitoring Set 12"	Edward Lifesciences	PX212
4-way stopcock	Edward Lifesciences	594WSC
Injection Site Interlink®	McKesson Medical	2N3399
6-0 Ethibond green 1x24" rb-4 double armed (surgical suture for suture retention test)	Ethicon	D9591
GlucCell Glucose Monitoring System	CESCO	DG1000
Glucose Test Strips	CESCO	DGA050
Instron 5960 mechanical testing system	Instron	N/A
SI-H KG7 Force Transducers	World Precision Instruments	N/A

LEAD CONTACT AND MATERIALS AVAILABILITY

Further information and requests for resources and reagents should be directed to and will be fulfilled by the Lead Contact, Dr. Yibing Qyang (yibing.qyang@yale.edu).

All unique/stable reagents generated in this study are available from the Lead Contact, Dr. Yibing Qyang, with a completed Materials Transfer Agreement.

EXPERIMENTAL MODEL AND SUBJECT DETAILS

Wild-type Human Induced Pluripotent Stem Cells

Human cell populations were derived using protocols approved by Yale University Human Investigation Committee. The previously established wild-type human induced pluripotent stem cell (hiPSC) line Y6 was employed in our research (Dash et al., 2016; Gui et al., 2016). Y6 hiPSCs were originally produced through reprogramming fibroblasts derived from discarded female neonatal skin tissue, under Yale Institutional Review Board approval, using Sendai viral particles that encode human OCT4, KLF4, SOX2, and c-MYC genes (ThermoFisher). To maintain the pluripotency, hiPSCs were expanded in mTeSR1 medium (STEMCELL Technologies) on Growth Factor Reduced (GFR)-Matrigel (Corning)-coated plates under feeder-free conditions at 37°C and were passaged every 5-7 days by Ethylenediaminetetraacetic acid (EDTA; ThermoFisher) treatment.

HLA-C-retained (CIITA-knockout) Human Induced Pluripotent Stem Cells

The human leukocyte antigen-C (HLA-C) retained (CIITA-knockout) hiPSC line (named as 585A1 hiPSCs in previously published study) was established via reprogramming peripheral blood mononuclear cells isolated from male donor by episomal vectors as previously described (Xu et al., 2019). These HLA-C-retained hiPSCs were expanded in mTeSR1 medium on GFR-Matrigel-coated plates under feeder-free conditions at 37°C and were passaged every 5-7 days by EDTA treatment.

Human Vascular Smooth Muscle Cells

Primary human vascular smooth muscle cells (VSMCs) derived from the aorta of male donors were purchased from Lonza. The primary human VSMCs were expanded in Smooth Muscle Growth Medium (SmGM-2; Lonza) on 0.1% (w/v) gelatin (Sigma-Aldrich)-treated culture dishes at 37°C and were passaged upon reaching 80% confluency by 0.05% trypsin-EDTA (ThermoFisher) treatment. To further induce the maturation phenotype of primary VSMCs for characterization of marker expression and contractile functions, primary VSMCs grown in SmGM-2 medium were subcultured in the VSMC maturation medium (Dulbecco's Modified Eagle Medium [DMEM; high glucose, ThermoFisher] with 1% [v/v] fetal bovine serum [Fetal Bovine Serum, FBS; Gemini], 2 mM L-glutamine [ThermoFisher], 1% [v/v] non-essential amino acid [NEAA; ThermoFisher], 1% [v/v] penicillin/streptomycin [pen/strep; ThermoFisher], 0.012 mM 2-mercaptoethanol [β-ME; ThermoFisher] and 1 ng/ml TGF-β1 [Peprotech]) for seven days.

Human Umbilical Vein Endothelial Cells

Human umbilical vein endothelial cells (HUVECs) derived from the umbilical cords of female donors were purchased from Lonza. The HUVECs were expanded in Endothelial Growth Medium (EGM-2; Lonza) on gelatin-treated culture dishes at 37°C and were passaged upon reaching 80% confluency by 0.05% trypsin-EDTA treatment.

Animal Use

NIH-Foxn1^{rnu} nude rats were obtained from Charles River Laboratories. All experiments were performed on male nude rats 10 weeks of age, weighing about 300 g. All procedures involving animal subjects were performed under the approval of the Institutional Animal Care and Use Committee (IACUC) of the Yale School of Medicine. All animal care complied with the NIH Guidelines for the Care and Use of Laboratory Animals.

Human Umbilical Arteries

Human umbilical cords (deidentified) were obtained from Yale–New Haven Hospital (New Haven, CT), delivered at 4°C, and processed immediately after delivery. Human umbilical arteries (HUAs) were then isolated from the umbilical cords (20–30 cm in length) within 30 minutes via sharp dissection in a sterile manner. A pair of Metzenbaum scissors were used to remove the Wharton's jelly surrounding the HUAs. The newly isolated HUAs were then gently washed with Dulbecco's Phosphate-Buffered Saline (PBS; ThermoFisher) containing penicillin 100U/mL and streptomycin 100 μg/mL (ThermoFisher) to remove blood clots and were immediately used for either biomechanical analysis or were subjected to histological analysis.

Porcine Coronary Arteries

The porcine coronary arteries were isolated from Yorkshire pigs (male, three-month-old) in 20 minutes after euthanization via Veterinary Clinical Services from Yale Animal Resources Center. Coronary arteries were immediately transferred to PBS containing penicillin 100U/mL and streptomycin 100 μg/mL (ThermoFisher) at 4°C. The adherent connective tissue and fat tissue were removed in a sterile manner, and the segments of arteries with inner diameters of approximately 3 mm were cut into vessel rings with 1-2 mm in length for evaluation of mechanical strength. The vessel rings from coronary arteries of three Yorkshire pigs were used to mechanical strength evaluation.

METHOD DETAILS

Generation of VSMCs from hiPSCs

The hiPSC-VSMCs were obtained via an embryoid body (EB)-based approach (Dash et al., 2016; Gui et al., 2016), with significant modifications (Figure S1A). Briefly, hiPSCs were expanded until 80% confluency and treated with 0.5 mM EDTA (ThermoFisher)

for 3 minutes at 37°C on Day 0. The dissociated cells (3 wells of a 6-well plate) were resuspended in mTeSR1 medium supplemented with 1:100 (v/v) GFR-Matrigel and 5 μM ROCK inhibitor (Y-27632; Millipore) and transferred to a 6-well low attachment plate (3 wells; Corning) for 24 hours, which allowed the formation of EBs with uniform size. The mTeSR1 medium (hiPSC self-renewal medium) was gradually mixed with EB medium (DMEM high glucose [ThermoFisher] supplemented with 10% FBS, 2 mM L-glutamine, 1% (v/v) NEAA, 1% (v/v) pen/strep, and 0.012 mM β-ME) in 2:1 (volume) on Day 1, 1:1 on Day 2 and 1:2 on Day 3, respectively. From Day 4 to Day 5, EBs were cultured with EB medium in suspension. EBs were then collected and seeded on a gelatin-coated culture dish for six days with EB medium. To induce VSMC lineage, the adherent EB-derived cells were dissociated by 0.05% trypsin-EDTA, re-seeded at 20,000 cells/cm^2 on a GFR-Matrigel-coated dish, and cultured in SmGM-2 medium until cells reached 80% confluence. This stage typically took 7-10 days, and these proliferative hiPSC-derived VSMCs were termed hiPSC-VSMCs-P. In order to expand hiPSC-VSMCs-P for vascular graft engineering, hiPSC-VSMCs-P were passaged to GFR-Matrigel-coated plates or flasks and cultured in expansion medium (DMEM supplemented with 10% [v/v] FBS, 2 mM L-glutamine, 1% [v/v] NEAA, 1 mM sodium pyruvate [ThermoFisher] and 1% [v/v] pen/strep) to "prime" the cells for an additional 1 or 2 passages. This led to the generation of hiPSC-VSMCs with effective proliferative potential while also expressing an enhanced level of VSMC markers and extracellular matrix proteins collagen I and III. The derivation of hiPSC-VSMCs for tissue engineered vascular graft (TEVG) generation typically took around four weeks.

To further induce the maturation phenotype of hiPSC-VSMCs (hiPSC-VSMCs-M) for characterization of marker expression and contractile functions, hiPSC-VSMCs-P grown in SmGM-2 medium were subcultured in the VSMC maturation medium (DMEM with 1% FBS, 1% [v/v] NEAA, 2 mM L-glutamine, 0.012 mM β-ME and 1 ng/ml TGF-β1) for seven days.

The lineage specific hiPSC-VSMCs (including hiPSC-VSMCs with embryonic origin of neuroectoderm, lateral plate mesoderm, or paraxial mesoderm) were derived following the chemically-defined method as previously reported (Cheung et al., 2012). The lineage specific hiPSC-VSMCs were subcultured in expansion medium (DMEM supplemented with 10% [v/v] FBS, 2 mM L-glutamine, 1% [v/v] NEAA, 1 mM sodium pyruvate and 1% [v/v] pen/strep) along with those hiPSC-VSMCs derived from our newly optimized EB-based method for comparison of proliferative capacity.

Immunostaining of Cultured Cells

Cells were washed with PBS and fixed in 4% paraformaldehyde (PFA; Electron Microscopy Sciences) for 10 minutes at room temperature (RT). The cells were then blocked in 10% normal goat serum (NGS; ThermoFisher) in PBST buffer (PBS with 0.3% Triton X-100 [Sigma-Aldrich]) for 30 minutes at RT. Subsequently, cells were incubated with the primary antibody in 1% NGS in PBST at 4°C overnight. Cells were washed again with PBS, incubated with secondary antibody (1:1000 in 1% NGS in PBST) for one hour at RT and washed with PBS again. Filamentous actin was stained with phalloidin (ThermoFisher) and the nuclei were counterstained with DAPI (ThermoFisher). All antibodies are listed in the Key Resource Table. Immunostained samples were analyzed using a fluorescent microscope (Leica). Fluorescence intensity (gray scale) of the markers in immunostained cells were analyzed with the ImageJ software and expressed relatively to cell number. Percentage of cells positive for the markers was quantified by using ImageJ software.

Quantitative Reverse Transcription PCR

Cells or engineered vascular tissues were subjected to RNA extraction and a quantitative reverse transcription PCR (qRT-PCR) assay to evaluate the gene expression of markers of interest. RNA extraction and purification were completed using the TRIzol RNA Isolation Kit (ThermoFisher), following the manufacturer's instructions. Subsequently, total RNA was subjected to reverse transcription using an iScript cDNA synthesis Kit (Bio-rad). The primer sequences of the genes used in qRT-PCR are listed in Table S1. qRT-PCR was performed using Bio-Rad IQ SYBR green supermix. Expression of genes of interest was normalized to that of human GAPDH. Three biological replicates were used for the analysis of each gene expression.

Cell Contractility Assay

hiPSC-VSMCs or human primary VSMCs cultured in either SmGM-2 medium, maturation medium (1% [v/v] FBS with 1 ng/ml TGF-β1 [Peprotech]), or TEVG medium (DMEM medium supplemented with 20% [v/v] FBS, 50 μg/mL ascorbic acid [Sigma-Aldrich], 50 μg/mL proline [Sigma-Aldrich], 20 μg/mL alanine [Sigma-Aldrich], 50 μg/mL glycine [Sigma-Aldrich], 3 ng/mL CuSO4 [Sigma-Aldrich], 0.13 U/mL human insulin [Sigma-Aldrich], 100 U/mL Penicillin G [Sigma-Aldrich] and 1 ng/mL TGF-β1 [Peprotech]) were treated with 1 mM carbachol (Abcam) or PBS (vehicle control) as a control for 20 minutes. Cell surface areas were recorded at the beginning and the end of the treatment. The changes of surface area were evaluated with the ImageJ software. Three independent batches of hiPSC-VSMCs or primary VSMCs were used in the contractility assay, and the changes in surface area of 10 randomly selected cells in each batch were recorded and analyzed, respectively.

MTT Assay

hiPSC-VSMCs derived from EB-based or chemically defined approach were seeded at 20,000 cells/well density into GFR-Matrigel-coated 96-well plates with expansion medium and cultured for three days. Cell proliferation was measured as a function of metabolic activity using 3-(4, 5-dimethylthiazol-2-yl)-2, 5-diphenyl tetrazolium bromide (MTT) (Sigma-Aldrich) on Day 4. MTT at 0.5 mg/ml was added into the medium of each well and incubated with the cells at 37°C for 2 hours, followed by cell solubilization with DMSO

(AmericanBIO) for 15 minutes. Absorbance was measured at 540 nm using the Synergy 2 multi-mode plate reader (BioTek). Three biological replicates were completed for evaluation of each cell group.

Culturing hiPSC-VSMCs on 5 mm x 5 mm PGA Scaffolds

The engineered vascular tissues were developed by seeding "primed" hiPSC-VSMCs onto PGA scaffolds, to evaluate the effect of growth factor components (TGF-β1 and PDGF-BB) in the TEVG medium (Figure 2A). Nonwoven-PGA polymer mesh (0.3 mm x 150 mg/cc, 20 cm x 30 cm sheet, Biofelt) was cut into small-size meshes (5 mm x 5 mm squares). The PGA squares were treated with 1.0 N NaOH (Sigma-Aldrich) for 1 minute, rinsed extensively with distilled water, sterilized with 70% ethanol, and air-dried overnight in a sterile manner. On the following day, PGA meshes were coated with 0.1% gelatin at 37°C for 1 hour, air-dried, and transferred into the 24-well low attachment dish (Corning).

"Primed" hiPSC-VSMCs cultured in the expansion medium (DMEM supplemented with 10% [v/v] FBS, 2 mM L-glutamine, 1% [v/v] NEAA, 1 mM sodium pyruvate [ThermoFisher] and 1% [v/v] pen/strep) were harvested, and 40 μL of the expansion medium containing 0.4 million hiPSC-VSMCs were dropped onto the PGA mesh and incubated at 37°C and 5% CO2 for one hour. The wells were then filled with 1 mL of expansion medium, and cells were cultured overnight at 37°C. On the following day, the medium was changed to the TEVG medium (DMEM medium supplemented with 20% [v/v] FBS, 50 μg/mL ascorbic acid [Sigma-Aldrich], 50 μg/mL proline [Sigma-Aldrich], 20 μg/mL alanine [Sigma-Aldrich], 50 μg/mL glycine [Sigma-Aldrich], 3 ng/mL CuSO4 [Sigma-Aldrich], 0.13 U/ml human insulin [Sigma-Aldrich] and 100 U/ml Penicillin G [Sigma-Aldrich]), supplemented with one of the following: 1) both human TGF-β1 (1 ng/ml, Peprotech) and human PDGF-BB (10 ng/ml, R&D system) (T/P), 2) TGF-β1 only (T/-), 3) PDGF-BB only (-/P), or 4) no growth factor (−/−). Medium was changed every other day. The tissues were cultured for 21 days and then harvested for both histological analysis and hydroxyproline assay.

Tissue Immunohistochemistry and Histology

Tissue samples were fixed in 4% PFA for three hours at RT and incubated in 15% (w/v) sucrose (Sigma-Aldrich) in PBS at 4°C for 16 hours. Subsequently, the fixed tissues were embedded in Tissue-Tek Optimal Cutting Temperature (OCT) Compound (Sakura Finetek) to develop the frozen blocks. Frozen blocks were sectioned at 5 μm intervals using cryostat (Leica CM1950) and the sections were stored at −80°C.

For immunostaining, slides were submerged in PBS for 10 minutes. Tissue sections were then incubated with PBST containing 10% NGS for 30 minutes at RT, and incubated with primary antibody in PBST containing 1% NGS at 4°C overnight in a humidified chamber. On the second day, sections were washed with PBS, incubated with secondary antibody (1:1000 in PBST with 1% NGS) for one hour at RT and washed with PBS again. Nuclei were counterstained with DAPI. Fluorescence intensity (gray scale) of positiveness of the markers in the total immunostained cells or HLA-A-positive cells were analyzed by using ImageJ software and expressed relatively to cell number. Percentage of positiveness of the markers in the HLA-A-positive cells were analyzed by using ImageJ software.

For hematoxylin and eosin (H&E) staining, Masson's Trichrome staining, Alizarin Red staining and elastic Verhoeff-Van Gieson staining (EVG staining), tissue sections were processed by Yale Pathology Tissue Services based on standard protocols.

TUNEL Assay

Tissue sections were processed according to the instructions from the TUNEL staining kit (Roche). DNA was counterstained by DAPI (ThermoFisher). Three biological replicates were completed for each group for statistical analysis of the percentage of TUNEL-positive cells. All immunofluorescence, histology and TUNEL staining micrographs were captured under an inverted microscope (Nikon Eclipse 80i).

Hydroxyproline Assay

The collagen weight of the vascular tissues or hiPSC-VSMCs cultured in Uniflex 6-well culture plates (Flexcell International Corporation) were determined by measuring the levels of hydroxyproline following the instruction of the hydroxyproline assay kit (Sigma-Aldrich). Collagen weight was then calculated based on the estimation that collagen contains approximately 10.0% hydroxyproline by weight (Dijkman et al., 2012; Piez and Likins, 1960). Three biological replicates were completed for each group.

Cell Culture with Pulsatile Uniaxial Stretch

The "primed" hiPSC-VSMCs expanded in DMEM containing 10% FBS, 2 mM L-glutamine, 1% NEAA, 1 mM sodium pyruvate and 1% pen/strep (or named as Gen 2 hiPSC-VSMCs-10% FBS in Figure S1) were seeded at 20,000/cm^2 onto the Uniflex 6-well culture plates coated with 0.5% (w/v) gelatin (Flexcell International Corporation) and cultured in the presence of the T/- or T/P TEVG medium for 48-hours. The plates were then either transferred to a FlexCell FX-6000T Tension System (Flexcell International Corporation) for uniaxial, pulsatile stretching (2.5% strain, 2.75 Hz, sinusoidal waveform, mimicking the stretching regimen for generating TEVG using human primary VSMCs [(Dahl et al., 2011)]), or maintained under static culture for an additional 48-hours. Next, 1 mL medium samples were immediately collected from each well to test the glucose consumption. Additionally, the central rectangular areas of the wells (stretched or static samples) were cut off with a scalpel, and immediately subjected to the subsequent experiments, including the qRT-PCR, immunostaining, hydroxyproline assay, and evaluation of cellular ATP concentration.

Evaluation of Glucose in Media

The medium samples prior to and after the hiPSC-VSMC culture in the presence or absence of a 48-hour stretching period via a FlexCell FX-6000T Tension System were collected. The amounts of glucose in media were next evaluated using GlucCell glucose monitoring system and glucose test strips (CESCO). The cell numbers in each experimental group were determined by cell counting. To calculate the glucose consumption rates, the changes of amount of glucose during the 48-hour culture period were normalized to the average cell numbers and the duration of culture of each experimental group (2 days). Three biological replicates were completed for evaluation of each experimental group.

Evaluation of Cellular ATP Concentration

To test the cellular ATP concentrations of hiPSC-VSMCs with or without 48-hour stretching via using FlexCell FX-6000T Tension System, the total ATP amounts were measured by using the colorimetric ATP assay kit (Abcam) according to the instruction. The cell numbers in each experimental group were determined by cell counting using a separated well of hiPSC-VSMCs in the same batch of culture under the same culture condition, and the total ATP amount was normalized to the average cell numbers to derive the cellular ATP concentration of each sample. Three biological replicates were completed for evaluation of each experimental group.

Generation of hiPSC-TEVGs

Small-caliber tissue engineered vascular grafts were derived by culturing hiPSC-VSMCs on PGA scaffolds as described previously (Dahl et al., 2011; Gui et al., 2016; Niklason et al., 1999). Fifteen million hiPSC-VSMCs were seeded onto tubular, 0.1% gelatin-coated PGA scaffolds which were sewn around silicon tubing (3.2 mm outer diameter; Saint-Gobain) and mounted inside sterilized glass bioreactors (Figure 3A). Vessels were cultured in 10% FBS expansion medium at 37°C, 5% CO_2 for 24 hours. The expansion medium was then replaced by the optimized TEVG medium (DMEM medium supplemented with 20% FBS, 50 μg/mL ascorbic acid, 50 μg/mL proline, 20 μg/mL alanine, 50 μg/mL glycine, 3 ng/mL CuSO4, 100 U/ml Penicillin G, 0.13U/ml insulin and 1ng/ml TGF-β1). Bioreactor medium (75%) was refreshed every two days. The engineered vessels were cultured without mechanical stimuli for the first week. Thereafter, pulsatile radial stress from a peristaltic pump (Cole-Parmer) was added incrementally, and the frequency of the mechanical stimuli was adjusted via the rotating speed of the peristaltic pump. The strain induced by the pulsatile radial stress started from 0.5% and was progressively increased to the desired maximum strain at the end of week 4 according to the experiment design. To generate the hiPSC-TEVGs with optimal mechanical strength, 3% of maximum strain was applied, and maintained at the maximum (3%) during the following 4 weeks of culture. By the end of week 8, hiPSC-TEVGs were harvested under sterile conditions for implantation and further analysis.

Implantation of hiPSC-TEVG into Nude Rat

hiPSC-TEVG segments were implanted as abdominal aorta interpositional grafts into 10-week-old, male NIH-Foxn1^{rnu} nude rats (around 300 g) (Charles River Laboratories). Nude rats were anesthetized with isoflurane, and subsequently opened under standard sterile conditions via a midline abdominal incision leaving the infrarenal abdominal aorta exposed. The cross-clamps were then applied to aid the removal of an aortic segment between the renal artery and the iliac artery. A hiPSC-TEVG segment (7-10 mm in length) was next implanted into the aorta in the "end-to-end" manner using a 10-0 monofilament nylon suture. After confirmation of blood flow and hemostasis following removal of the clamp, the wound area was closed. The animals were left to recover from surgery and maintained for 30 days or 60 days after surgery.

Ultrasonographical Assessment of Grafts

Nude rats were examined using a Vevo 770® Micro-ultrasound System (Visual-Sonics, Toronto, Canada) equipped with the RMV-704 scanhead (spatial resolution 40 mm) to determine patency and morphometry of the implanted hiPSC-TEVGs. The inner diameters and outer diameters of the grafts at the midpoint were measured from both transverse and longitudinal axis ultrasound images. The lengths of the grafts were measured from longitudinal axis ultrasound images. The average wall thickness of the midpoint of the implanted grafts was calculated as half of the difference between the outer and inner diameters. For TEVG 1-6, the implanted hiPSC-TEVGs were ultrasonographically analyzed on Day 7, Day 14, Day 21 and Day 28 post-implantation and explanted for histological analysis on Day 30. For TEVG 7, the graft was ultrasonographically analyzed on Day 7, Day 14, Day 21, Day 28, Day 35, Day 42, Day 49 and Day 56 post-implantation and explanted for histological analysis on Day 60.

Mechanical Evaluation of hiPSC-TEVGs

The suture retention strength and rupture pressure of hiPSC-TEVGs were determined as previously described (Gui et al., 2016), and HUAs were utilized as a control. Suture retention strength was evaluated by adding weights on a loop of 6-0 Prolene suture (Ethicon) threaded through one side of the TEVG wall, 2 mm from the end, with force applied axially to the graft. The weights were augmented in 10 g to 20 g increments until failure. Four biological replicates were completed for either hiPSC-TEVG or HUA. To measure rupture pressure, vessel segments of 1-1.5 cm long were connected to a flow system coupled with a pressure transducer. PBS was injected into the flow system until vessel rupture. Four biological replicates were completed for either hiPSC-TEVG or HUA.

The maximum modulus, maximum tensile stress and failure strain of pre-implanted and explanted hiPSC-TEVGs were analyzed using an Instron 5960 microtester (Instron) equipped with a 10 N load cell as previously described (Luo et al., 2017). The porcine coronary artery segments with inner diameters of approximately 3 mm were employed as control. The hiPSC-TEVGs or porcine coronary

arteries were cut into vessel rings with 1-2 mm in length. The vessel rings were mounted between two stainless steel pins, with one anchored to actuator and the other to the load cell. Vessel rings were next cyclically pre-stretched for three cycles to 10% strain and then increasingly stretched until failure to determine the ultimate tensile strength. Tissue stress was quantified by normalizing tensile force to total cross-sectional area ($A = 2 * \pi * r^2$; supposing ring cross section to be circular, r is half of the ring thickness, and cross-sectional area of the ring is multiplied by two to include both sides of the ring), and then the maximum stress, failure strain, maximum modulus of the rings were calculated and plotted. Three independent batches of pre-implanted hiPSC-TEVGs, explanted hiPSC-TEVGs or porcine coronary arteries were subjected to mechanical property evaluation and analyzed.

Contractility Evaluation of hiPSC-TEVGs

The contractility of the hiPSC-TEVGs was measured as previously described (Luo et al., 2017). Briefly, the vessel rings (1-2 mm in length) of pre-implanted or explanted hiPSC-TEVGs 30 days after implantation were sectioned and transferred into a temperature-controlled perfusion bath as shown in Figure S3P. Vessel rings were hooked between two motorized micromanipulators, which kept the ring suspended between an anchoring point and a force transducer (KG7, SI Heidelberg). When measuring the force, rings were placed in freshly bubbled Tyrode's solution (NaCl 140 mM, KCl 5.4 mM, $MgCl_2$ 1 mM, HEPES 25 mM, glucose 10 mM and $CaCl_2$ 1.8 mM, pH 7.3, all from Sigma-Aldrich) at 37°C. Force were measured at the original length, and the manipulators were then moved apart 1.5 mm to evaluate the second reference force prior to stimulation of agonist. The vessel rings were kept untreated for one minute to achieve a baseline value for force change, and then carbachol solution was immediately added to the bath at 1 mM to induce contraction of the ring. The force measurements of vessel rings were recorded for 30 minutes using a Customized MATLAB software. The ultimate changes in tension (Pa) were quantified by normalizing the force by the cross-sectional area. The areas of cross-section were derived using optical coherence tomography (Ganymede-II- HR, Thorlabs). An index of refraction of 1.38 was employed for each vessel ring. Images were taken, and their cross-sectional area was quantified by using the NIH ImageJ software and averaged to calculate the overall cross-sectional area of the vessel rings. Three independent batches of pre-implanted hiPSC-TEVGs or explanted hiPSCs were subjected to contractility tests and analyzed.

QUANTIFICATION AND STATISTICAL ANALYSES

All graphic illustrations and statistical analyses were completed using GraphPad Prism 6. One-way or two-way ANOVA followed by Tukey post hoc test was applied for comparison among multiple groups when appropriate. Two-tailed Student's t test was used to determine the significance of difference between the controls and the experimental groups. A p value lower than 0.05 was considered significant. Numerical data were reported in format of mean ± SEM from at least three or more independent experiments. The sample size (n) for each analysis stands for the number of biological replicates and can be found in the figure legends. The statistical details of each experiment can also be found in figure legends and related results.

DATA AND CODE AVAILABILITY

Main data have been listed in the primary figures and supplemental information. All the original data and images are available from the Lead Contact upon request.